Pergamon

Cement and Concrete Research 33 (2003) 689–696

CEMENT AND CONCRETE RESEARCH

Study of the water-retention capacity of a lime–sand mortar: Influence of the physicochemical characteristics of the lime

Y. Sébaïbi, R.M. Dheilly, M. Quéneudec*

Laboratoire des Transferts et Réactivité dans les Milieux Condensés, Université de Picardie Jules Verne, I.U.T. d'Amiens—Département Génie Civil, Avenue des Facultés, 80025 Amiens, Cedex 1, France

Received 15 August 2002; accepted 22 October 2002

Abstract

The purpose of this study is to evaluate the influence of limes' characteristics on the water-retention capacity of a lime–cement–sand mortar. Toward this aim, various categories of lime were partially substituted for the cement Portland CEM I 52.5 in mortars. The total binder/sand ratio has been maintained constant.

Experimental results have highlighted the combined influence of both lime characteristics and lime content.

As the proportion of lime in the mix increases the results demonstrate that the action of lime in a cement–lime mortar must not be analysed in terms of morphology and chemical nature alone. However, the electrical phenomena capable of being generated must be taken into account.

Keywords: Mortar; Portland cement; $Ca(OH)_2$; Pore size distribution; Water-retention capacity

---

1. Introduction

Masonry coatings are submitted to thermal and hydric constraints, which contribute heavily to their ageing. When mixing, water evaporates too quickly or gets absorbed by the support material. This can actually induce insufficient hydration of the cement, and thus a decrease in mechanical strength, which in turn is capable of increasing the sensitivity of the coating to both spalling and cracking. Determination of the water-retention capacity of the mortar is therefore a key element behind the choice of coating as a function of climatic conditions and state of the support material, toward the aim of facilitating coating workability and preserving its durability.

It is widely accepted that although lime does not serve to enhance coating strength, it does contribute considerably to water-retention capacity [1].

Nevertheless, the general term "lime" spans a large number of industrial products [2] that may be differentiated by their chemical composition and level of hydration. These characteristics are capable of influencing the behaviour of lime-based products, both in an aqueous environment and in the presence of cement. For this reason, the present work has focused on the influence of lime characteristics as regards the water-retention capacity of a lime–sand mortar. The types of lime studied herein are calcic or magnesian slaked limes, hydrated in accordance with various processes. The influence of both lime characteristics and the lime content in the mortar were analysed, especially in terms of pore structure and chemical composition.

2. Materials and experimental set-up

2.1. Raw materials

2.1.1. The cement (Ce)

The cement used is CPA CEM I 52.5 (EN 196-1), which contains more than 95% clinker. Its specific surface area is 1.66 m^2/g. Fig. 1 shows that this cement features laser-based gap grading that extends from 0.04 to 100 μm and displays two maxima: one at 0.3 μm, the other at 20 μm.

Its chemical analysis and Bogue composition are listed in Table 1.

---

* Corresponding author. Tel.: +33-3-22-53-40-16; fax: +33-3-22-53-40-96.

E-mail address: Michele.Tkint@iut.u-picardie.fr (M. Quéneudec).

0008-8846/02/$ – see front matter © 2002 Elsevier Science Ltd. All rights reserved.
doi:10.1016/S0008-8846(02)01038-4

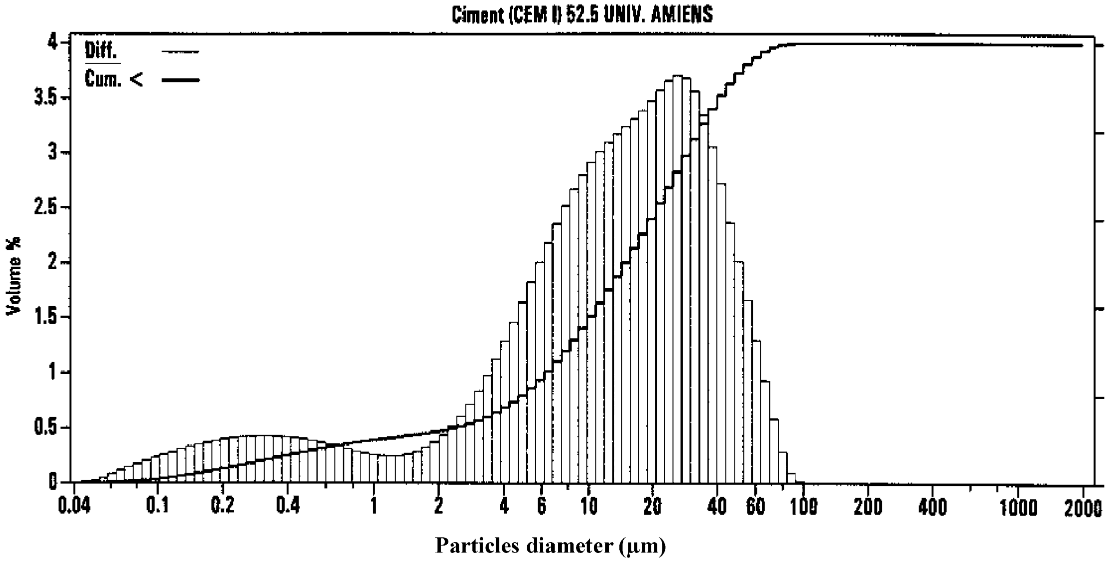

Fig. 1. Gap-grading analysis of the cement.

2.1.2. The sand (S)

It is a siliceous sand commonly encountered as a building material in the northern French region of Picardy. EDX-analysis displays the presence of a few nonsiliceous components (Fig. 2), whereas scanning electron analysis reveals the angular shape of the grains.

2.1.3. Limes (Ci)

The main characteristics of the grading curves for the various limes used in this study are presented in Table 2, and their physicochemical characteristics (chemical composition, specific surface area and laser-based gap grading) are listed in Table 3.

The calcium and magnesium hydroxides used in this study are pure hydroxides (i.e., of analysis-grade quality). Their purities are greater than 98% and 95%, respectively. On a scanning electron micrograph, both $Ca(OH)_2$ and $Mg(OH)_2$ appear as a cluster of fine platelets measuring up to 10 μm in the case of calcium hydroxide, yet whose entanglement makes it impossible to define the exact shape (Fig. 3a and b).

The industrial limes studied herein (C_1, C_2 and C_3) are slaked limes chosen for the diversity of their physicochemical characteristics.

Limes C_1 and C_2 were hydrated under atmospheric pressure (Fig. 3c and d); their composition and purity are close to those of calcium hydroxide. They exhibit the same morphology as calcium hydroxide. In the case of C_2, however, the tablets exhibit a smaller size. While the specific surface area of C_1 is close to that of $Ca(OH)_2$, such is not the case for lime C_2. The specific surface area of this lime turns out to be 2.65, which is as high as that of calcium hydroxide.

Lime C_3 is a dolomite (Fig. 3e), which has been hydrated under pressurised conditions [3,4]. This category of lime differs from lime hydrated under atmospheric pressure by the presence of a small proportion of non-

Table 1
Chemical analysis and Bogue composition of the CPA CEMI cement used in mortar production

CaO	MgO	SiO_2	Fe_2O_3	Al_2O_3	SO_3	LI 1000 °C	C_3S	C_2S	C_3A	C_4AF
64.8	0.8	21.3	4.3	3.7	2.7	1.2	62.0	14.0	2.5	13.1

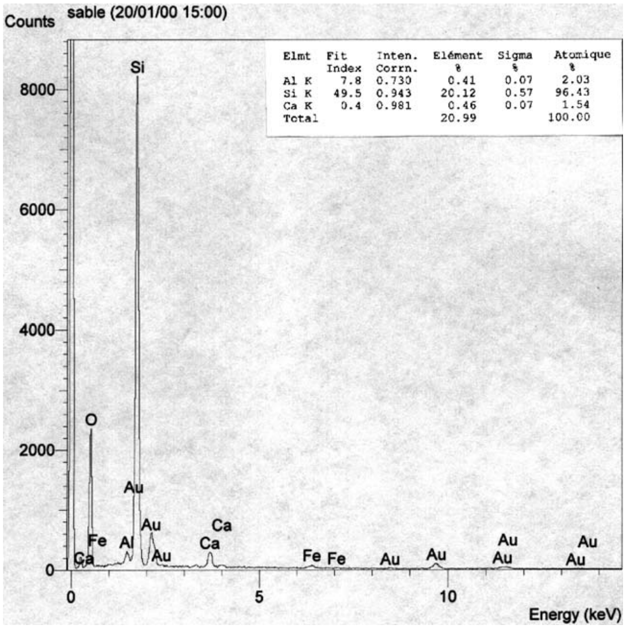

```
Elmt   Fit    Inten.  Elément  Sigma   Atomique
       Index  Corrn.    %        %        %
Al K     7.8  0.730     0.41    0.07     2.03
Si K    49.5  0.943    20.12    0.57    96.43
Ca K     0.4  0.981     0.46    0.07     1.54
Total                  20.99            100.00
```

Fig. 2. EDX-analysis of the sand that has been used for the mortar production. In order to facilitate observation, this sample was covered with a thin layer of spray-on gold.

Table 2
Laser-based gap grading and shape of the grading distribution for the various limes tested

	$Ca(OH)_2$	$Mg(OH)_2$	C_1	C_2	C_3
Grading distribution (μm)	0.1–80	0.15–80	0.1–200	0.4–1000	0.2–200
Maxima	4 μm	40 μm	6 μm	3 μm + little maximum at 600 μm	2 μm
Stages	10 to 60 μm	1.5 to 20 μm		10 to 60 μm	10 to 200 μm

hydrated oxides (< 8%), high plasticity, and a high water-retention capacity (which may be attributed to the small size of the crystals (< 1 μm)).

Although lime C_2 is constituted of larger size crystals, this lime exhibits a specific surface area more important than those of the other limes. This phenomenon can be related to its more important porous volume.

Lime C_4 (Fig. 3f) is a laboratory-made mix containing the aforementioned pure "analysis-grade" magnesium and calcium hydroxides, which were mixed in the same proportions as those of sample C_3 [55% $Ca(OH)_2$ and 45% $Mg(OH)_2$]. Limes C_3 and C_4, whose chemical compositions are similar, appear on scanning electron analysis as a cluster of fine particles composed of both $Ca(OH)_2$ and $Mg(OH)_2$. In the case of industrial lime C_3, which has been hydrated under pressure, this cluster appears to be more compact. Even if qualitative analyses were performed, it would be difficult to differentiate the platelets of calcium hydroxide from those of magnesium hydroxide. The specific surface area of this lime is 2.5 times higher than that of C_4.

As regards the incremental volumic distribution (see Fig. 4), it appears that limes C_1 and C_2 are very close to one another over the range of small-dimension pores. Lime C_2 shows two very distinct maxima, one centred at 45 Å and the other at 120 Å. For limes C_3 and C_1, these same maxima exist, yet are lower and slightly displaced (i.e., centred at 100 and 85 Å, respectively). Although C_3 displays maxima at 40, 100 and 300 Å, it has the most uniform pore distribution over the studied domain.

The cumulative volume curve (Fig. 5) shows that the lime with the highest proportion of pores less than 100 Å is C_2. This proportion is slightly lower for C_3 and considerably lower for the other limes [especially $Mg(OH)_2$]. Above 150 Å, the cumulative proportions of pores is the inverse for limes C_3 and C_2. Regardless of pore diameter, C_4 presents much lower cumulative volumes than C_3.

2.2. Experimental set-up

This work has focused, for the most part, on a single characteristic of the fresh material, i.e., the one necessary for workability: water retention of the mortar.

2.2.1. Mortar production

The mortars were prepared in accordance with the mass proportions for sand and binder stipulated in Standard EN 196-1 regarding "normal" mortars (i.e., S/B = 3). Mixing of the various components was performed in a standardised mortar mixer (again in accordance with EN 196-1). This mixer operates with an orbital movement and at two speeds (62.5 ± 5 and 125 ± 10 rpm).

2.2.2. Determination of water retention

This test is conducted with a standardised apparatus (in accordance with ASTM C.91) in the presence of a 50-mm mercury (Hg) depression applied for a period of 15 min. The test procedure complies with those presented in the CSTB organisation's classification of monolayer coatings and waterproofing [5].

Prior to testing, the dish, which had been fitted with a humidified and drained filter paper, is filled with mortar, levelled and weighed (mass denoted M_2). Knowing the mass of the empty dish with the humidified filter paper (mass M_1), mass M of the mixed and placed product can therefore be calculated, along with mass E of the mixing water (these results are given in grams).

Measurements are to be undertaken within 10 min following mixing. A vacuum is created for a 15-min period at a time

Table 3
Physicochemical characteristics of the various limes tested

Samples	$Ca(OH)_2$	$Mg(OH)_2$	C_1	C_2	C_3	C_4^a
Ca0	74.2	0.1		73.9	42.3	
Mg0	0.7	68.2		0.6	29.8	
Fe_20_3	0.06	< 0.01		0.3	0.1	
$Si0_2$	0.10	0.08		0.3	0.4	
Al_20_3	0.08	< 0.01		0.1	0.1	
S	< 0.01	< 0.01		0.03	0.04	
$LI_{1000\ °C}$	24.8	31.1		24.3	26.7	
$Ca(OH)_2$ (%)	97.4		94.4	96	55.2[b]	
$Mg(OH)_2$ (%)		98.5[b]				
Specific surface area (BET), (m^2/g)	15.5	6.6	17.5	41.2	28.8	11.4
Grading distribution						
1 μm	10	11	9	5	12	10
5 μm	52	37	44	38	58	52
10 μm	69	48	68	52	69	66
20 μm	82	60	85	65	78	77
32 μm	90	71	91	74	84	85
45 μm	95	89	94	80	88	93
63 μm	99.5	99.4	96	85	92	99
90 μm	99.9	100	98	90	95	100
160 μm	100	100	99.9	95	99.5	100
250 μm	100	100	100	98	100	100
500 μm	100	100	100	99	100	100

[a] The sample C_4 is a laboratory-made mix containing pure "analysis-grade" calcium and magnesium hydroxides in the same proportions as those of a hydrated dolomite [55% $Ca(OH)_2$ and 45% de $Mg(OH)_2$].

[b] Value obtained by thermogravimetric analysis.

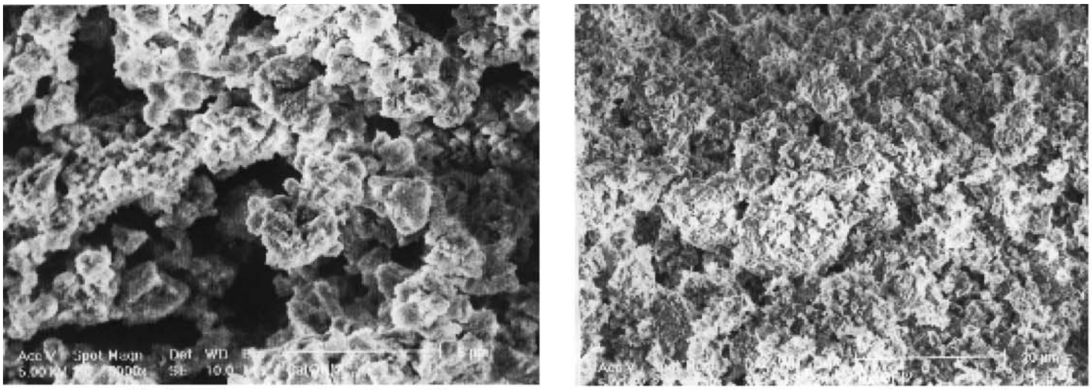

a : $Ca(OH)_2$ pure hydroxide **b : $Mg(OH)_2$ pure hydroxide**

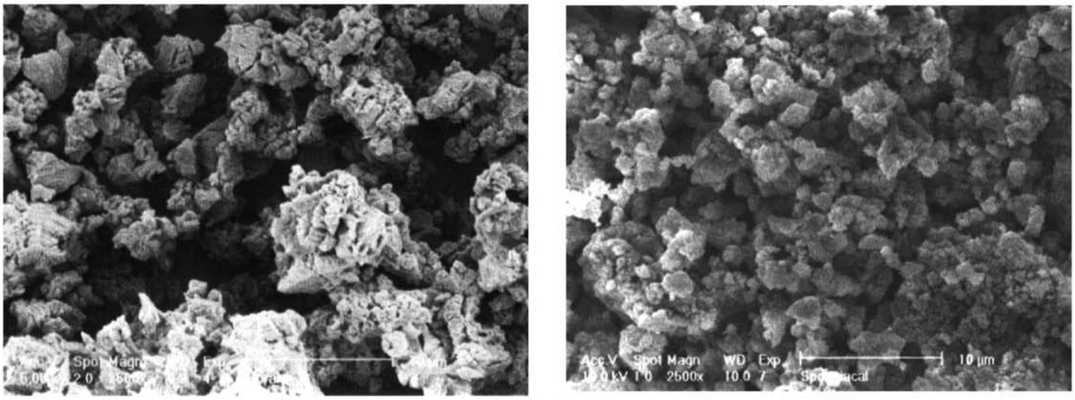

c : C_1 **d : C_2**

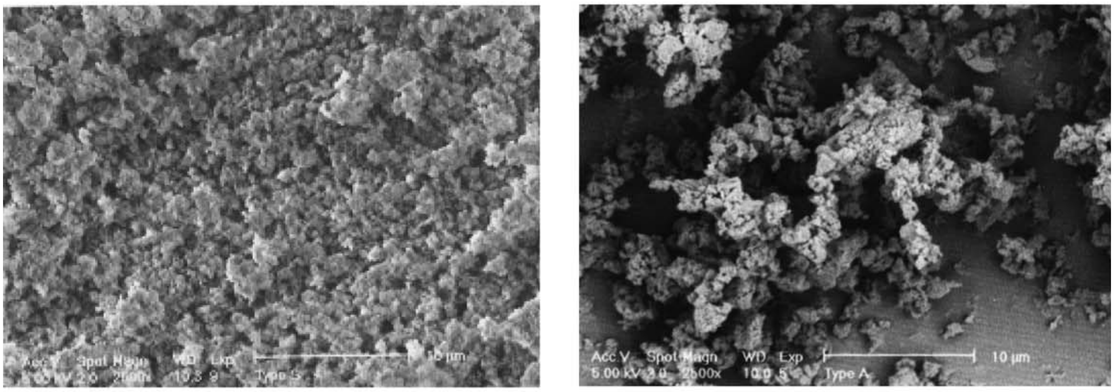

e : C_3 **f : C_4**

Fig. 3. Scanning electron migrographs of pure calcium and magnesium hydroxides and of studied industrial limes ($G = 2500$).

of 15 min after mixing has begun. The apparatus is then exposed to a 50-mm Hg depression. Once the underface has been dried, the dish is reweighed. By taking differences, the water loss e is determined (in grams).

The water-retention capacity is expressed by relationship (1) in terms of percentage of initial mixing water mass:

$$\frac{E-e}{E} \times 100 \tag{1}$$

2.2.3. Scanning electron microscopy

Scanning electron micrographs have allowed visualisation of the morphology of materials used in these tests and then identification of the different phases present in the mortar. This analysis has, in particular, made it possible to visualise the arrangement of the various species present in the mortar paste.

In order to facilitate observation, the samples were dried beforehand and then covered with a thin layer of spray-on gold. The micrographs were generated with a PHILIPS FEG XL 30, which allows conducting both a qualitative and

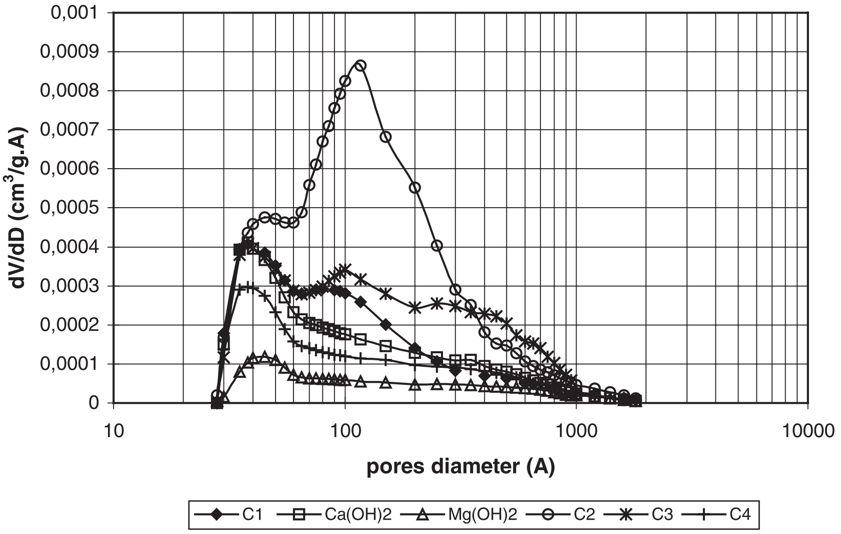

Fig. 4. Incremental volumic distribution of the various limes.

quantitative X-analysis of the samples during the observation period.

2.2.4. Morphological analysis

The raw materials were characterised by use of a laser granulometry technique. Measurements were performed on a Type 850 CILAS diffraction laser; this device enables analysis over the 0.1- to 600-μm range.

For the surface area and porosity measurements, a Micrometrics ASAP 2010 (with nitrogen) was used. The surface area of samples was determined by means of the BET method [6]. BET calculations provide the value of the sample surface area by determining the monolayer volume of adsorbed gas from the isotherm data. The BJH method was employed to obtain additional information on the pore distribution and volume of the various samples [7]. This measurement also allows determination of the pore volume and mass density of pores whose radii fall between r and $r + dr$.

3. Experimental results and discussion

In order to develop a number of different mortars, cement has been replaced by various types of limes using a range of lime proportions; moreover, the workability of these mortars has been held constant. The water quantities used have thus been adjusted to obtain a mortar consistency, whereby the proportions by weight are: Ce/S = 1/3 with W/Ce = 0.5 where Ce = cement, S = sand and W = water.

3.1. Influence of lime characteristics

The substituted lime percentage is held constant at 2% of total binder mass *B*. This quantity corresponds to an optimal mechanical characteristic value [8]. The various W/B ratios obtained, as well as water-retention values for the mortars, are listed in Table 4.

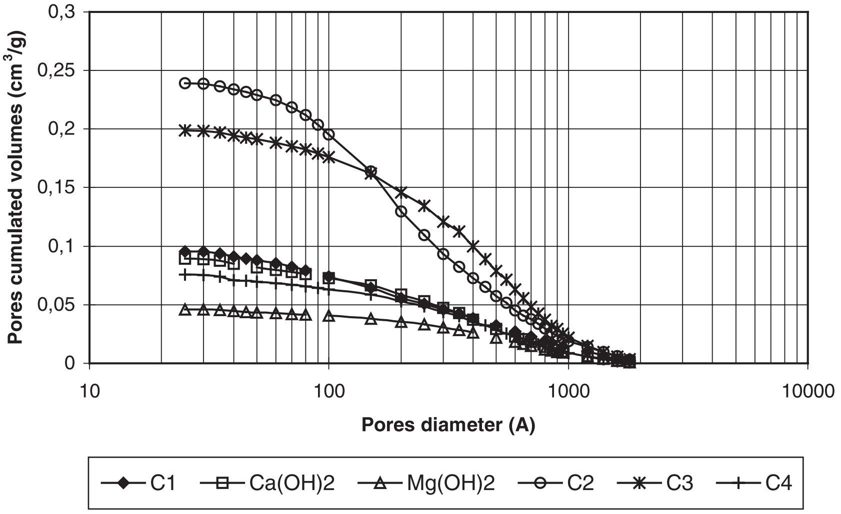

Fig. 5. Cumulative pore volumes of the various limes.

Table 4
Water-retention values obtained for various mortars with 2% lime substituted for cement at an equal level of consistency

Sample	"Normal" mortar	Mortar with $Ca(OH)_2$	Mortar with $Mg(OH)_2$	Mortar with C_1	Mortar with C_2	Mortar with C_3	Mortar with C_4
W/B ratio	0.500	0.500	0.500	0.510	0.500	0.525	0.500
Water retention (%)	77.60	86.74	81.55	83.56	79.14	84.32	84.74

Fig. 6 shows the evolution in water retention as a function of both the specific surface area (Fig. 6a) and total pore volume (Fig. 6b). The linear relationship (Fig. 7) derived between specific surface area and pore volume explains the similarity of these curves. It can be observed that this retention is not an increasing function of either specific surface area or total pore volume.

It thus seems that the pore morphology must be taken into account.

For example, if lime C_1 and $Ca(OH)_2$ are compared, it can be noted that they possess practically the same specific surface area. In contrast, the volume of pores whose diameter lies between 60 and 300 Å is proportionally higher in the case of C_1, which induces less water retention than $Ca(OH)_2$.

More generally, in the case of calcic limes, water retention drops as the volume of 60–300 Å pores increases, i.e., $Ca(OH)_2 < C_1 < C_2$. In the case of magnesian limes, the increase in this pore volume is such that $Mg(OH)_2 < C_4 < C_3$, which corresponds to a slight increase in water retention. The influence of pore morphology, therefore, is different depending on the chemical nature of the lime. In this respect, it can be observed that limes C_3 and C_4, which display the same proportions of $Mg(OH)_2$, also induce the same water-retention level despite their

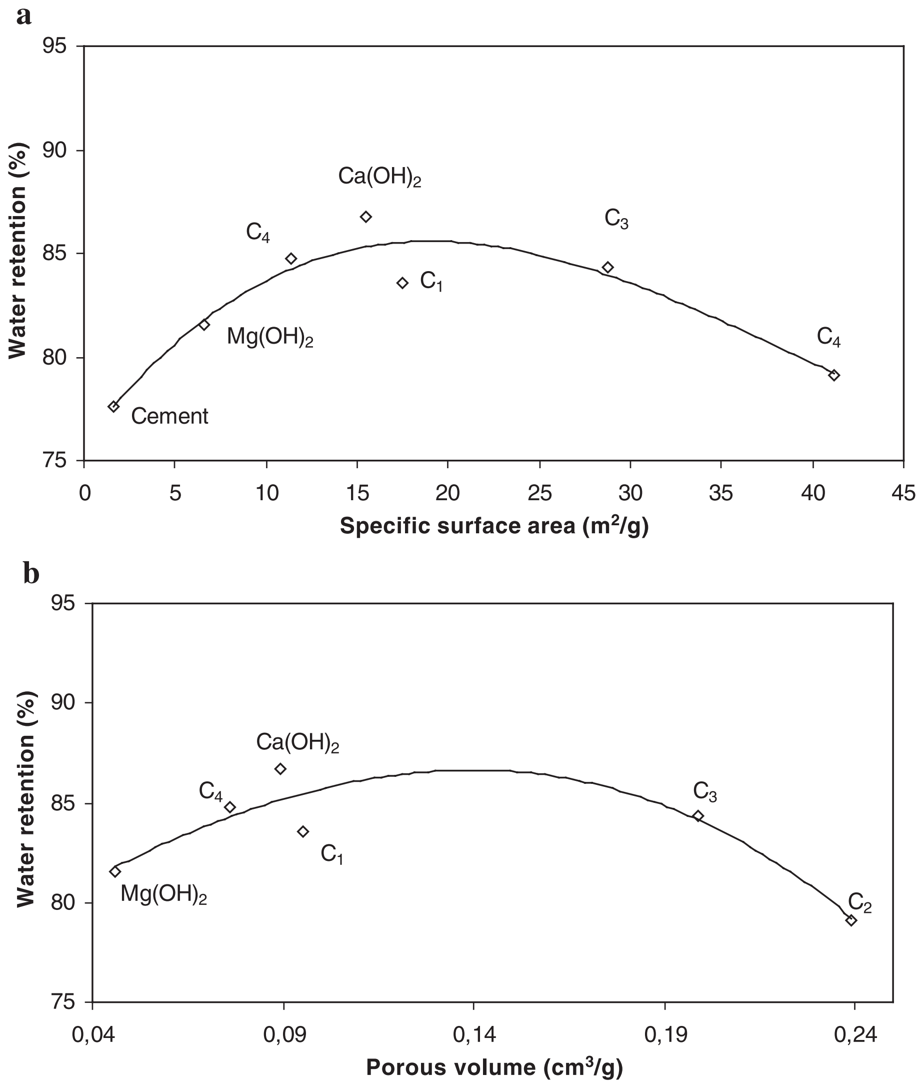

Fig. 6. Evolution of water retention as a function of the specific surface area (a) and of the total porous volume (b).

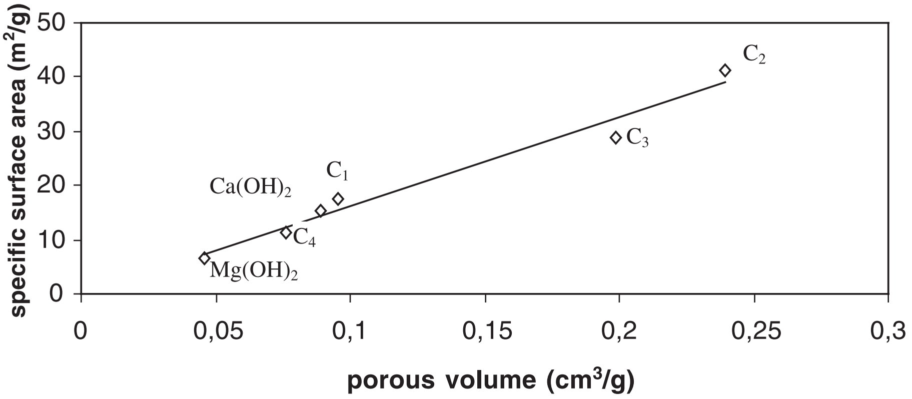

Fig. 7. Evolution of specific surface as a function of the total porous volume.

differing specific surface areas, pore volumes and crystalline shapes.

Hence, in the mortars studied, water retention is not dependent on specific surface area, but rather on both pore morphology and the chemical nature of the lime. These two effects cancel each other out.

3.2. Influence of the percentage of substituted lime

In this section, an average water quantity that provides for easier pouring of the paste has been used, i.e., W/B = 1. In all cases, the binder/sand ratio remains constant and equal to 1/3. The quantity of cement-substituted lime is the sole variable. Under these conditions, in the absence of lime, water retention is close to 80%.

As the total lime/binder percentage Ci/(Ci + Ce) varies from 0% to 100%, all of the curves obtained reach a minimum, subsequent to which water retention increases again. Fig. 8 shows the case of limes C_1 and C_2.

The percentage of cement-substituted lime that yields minimum water retention differs from one lime to the next. The values obtained for each type of cement-substituted lime are listed in Table 5. Fig. 9 indicates the evolution in lime content corresponding to the minimum retention level as a function of both specific surface area and total pore volume of the cement-substituted lime.

Fig. 9 reveals that the percentage of lime corresponding to minimum water retention varies in a nonlinear manner with both specific surface area and total pore volume. No direct relationship is observed between the percentage of lime at the minimum retention level and the quantity of retained water, nor can a direct relationship be observed between the quantity of retained water at minimum retention and the morphology of the lime. Similarly, the chemical nature alone cannot explain this variation in minimum retention.

For example, limes C_3 and C_4, which contain the same chemical species in the same proportions, feature minima of approximately 35% and 48%, respectively. These minima

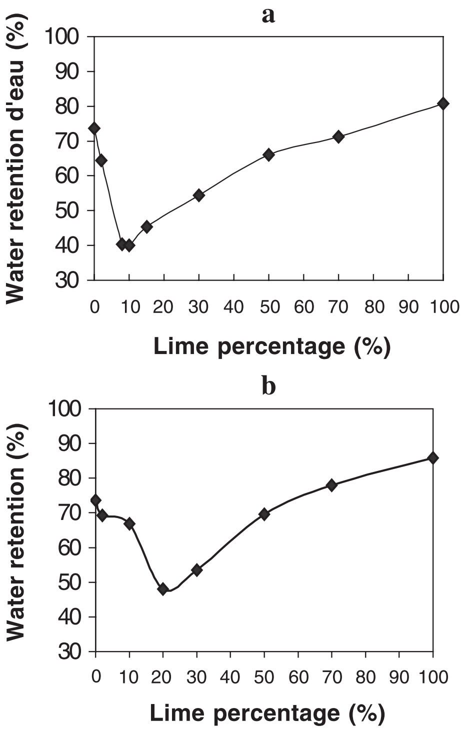

Fig. 8. Evolution of water retention as a function of the lime percentage: lime C_1 (a) and lime C_2 (b).

Table 5
Influence of type of lime on water retention

	Type of substituted lime					
	$Ca(OH)_2$	$Mg(OH)_2$	C_1	C_2	C_3	C_4
Specific surface area (m^2/g)	15.5	6.6	17.5	41.2	28.8	11.4
Porous volume (cm^3/g)	0.0893	0.0459	0.0954	0.2392	0.1988	0.0760
Water retention with 100% lime	100	85.22	80.74	85.85	92.5	80
Minimum water retention (%)	67.3	61.85	40.1	45.08	34.5	47.51
Percentage of lime at this minimum	8	12	10	20	12	10

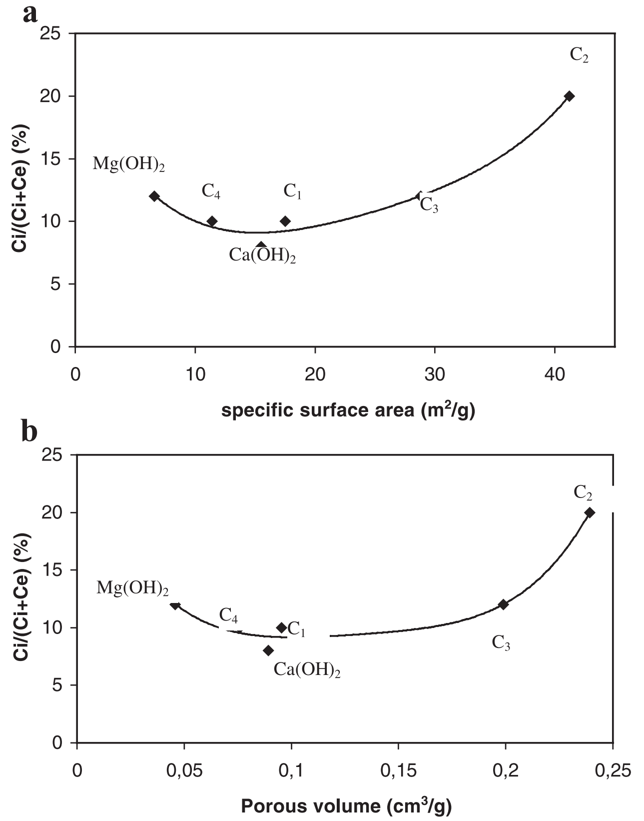

Fig. 9. Evolution of the lime/binder percentage Ci/(Ci + Ce) corresponding to minimum water retention as a function of the specific surface area (a) and of the total porous volume (b).

are inversely proportional to the specific surface area of the two limes. Moreover, lime C_1 and $Ca(OH)_2$, of approximately the same chemical composition and specific surface area, exhibit curves whose minima are positioned at 40% and 67%, respectively.

This minimum value is not correlated with the observed water-retention level for a 100% lime mortar. In the case of lime C_3, the mortar (which contains exclusively lime as a binder) shows a very high retention rate: 92.5%. In contrast, minimum retention stands at just 35% for a mortar with 12% lime content. Both lime C_2 and magnesium hydroxide induce mortars that display approximately the same retention, although the specific surface areas and pore volumes are different. The minima values, however, differ markedly: 45% and 62%, respectively.

As lime content increases, it is necessary to take into account the interactions occurring between these various limes, the cement and the mixing water. These interactions promote the flocculation of solid particles that entrap air and water, to varying extents and with varying degrees of efficiency. This grouping of solid particles, under the influence of a number of distinct forces, is dependent upon both capillary tension and the charges present on the surface of particles, i.e., not only specific surface area, but also the crystalline structure and solid-grain morphology. Needless to say, the phenomenon involved is very complex.

4. Conclusion

The objective of this work has been to study the influence of lime on the water-retention capacity of a lime–sand mortar. Various categories of lime and lime proportions have been tested using a constant total binder/sand ratio. Experimental results have allowed highlighting the combined influence of chemical nature and lime morphology.

In the case of low lime content, which corresponds to optimal mechanical strength, hydrous exchanges are related to both the specific surface area and total lime porosity; mesoporosity, however, does seem to play an essential role. As the proportion of lime in the mix increases, the rearrangement of particles exposed to the complex interaction effect must be taken into account. These results demonstrate that the action of lime in a cement–lime mortar must not be analysed in terms of morphology or chemical nature alone, but instead must consider the electrical phenomena capable of being generated.

References

[1] S. Tsimas, K. Raikos, Lime an irreplaceable mortar constituent, ZKG Int. 48 (6) (1995) 350–356.
[2] Standard Specification for Hydrated Lime for Mansonry Purposes, ASTM Designation C 206-84 (1992) 168–169.
[3] J.A.H. Oates, Lime and limestone, Chemistry and Technology, Production and Uses, Wiley-VCH, New York, 1998, pp. 208–225.
[4] R.S. Boynton, Chemistry and Technology of Lime and Limestone, 2nd ed., Wiley, New York, 1966.
[5] Certification CSTB des enduits monocouches d'imperméabilisation, Classification MERUC, Cahiers du CSTB, CSTB, Paris, 1993, pp. 2669–2663.
[6] S. Brunauer, P.H. Emmet, E. Teller, Adsorption of gases in multimolecular layer, J. Am. Chem. Soc. 60 (1938) 309–319.
[7] E.P. Barret, L.G. Joyner, P.P. Halenda, The determination of the pore volume and area distributions in porous substances: I. Computations from nitrogen isotherms, J. Am. Chem. Soc. 73 (1951) 373–380.
[8] Y. Sebaïbi, Influence d'une chaux magnésienne de type "S" sur les propriétés d'un mortier de ciment Portland, Comparaison avec d'autres chaux, Thesis, INSA de Lyon, Lyon, 2000.